

## Effect of crystallinity and surface silanol groups on rheological properties of different sepiolites

Mustafa Çınar <sup>1</sup>, İlhan Gülgönül <sup>2</sup>, Orhan Ozdemir <sup>3</sup>, Mehmet S. Çelik <sup>4,5</sup>

<sup>1</sup> Çanakkale Onsekiz Mart University, Mining Engineering Department, 17400, Canakkale, Turkey

<sup>2</sup> Balıkesir University, Mining Department, Balıkesir, Turkey

<sup>3</sup> Istanbul University-Cerrahpasa, Mining Engineering Department, 34500, Buyukcekmece, Istanbul, Turkey

<sup>4</sup> Istanbul Technical University, Mineral Processing Engineering Department, 34469, Maslak, Istanbul, Turkey

<sup>5</sup> Harran University, Rectorate, Şanlıurfa, Turkey

Corresponding author: [mcinar@comu.edu.tr](mailto:mcinar@comu.edu.tr) (Mustafa Cinar)

**Abstract:** In this study, differences in the rheological properties of three different types of brown sepiolites (K1, K2, and K3) along with one beige (B) sepiolite with different physicochemical properties were explained based on their crystallinity and level of surface silanol groups. Towards this aim, SEM images, XRD and chemical analyses, cation exchange capacity (CEC), and water absorption tests were conducted along with surface area measurements and time-dependent pH profiles. The pH profiles at 3% by wt. revealed that each sepiolite sample attained the equilibrium at different times. These differences showed a parallel behavior with the degree of crystallinity. While sepiolite with better crystallinity (K1) was rather slow in reaching the equilibrium pH, the sepiolites with poor crystallinity (B and K3) reached their equilibrium pH more quickly. The rheological studies conducted with different sepiolites at 3% solids concentration exhibited time-dependent flow of the Bingham plastic model and thixotropic. Differences observed in the rheological behavior of sepiolites were found to correlate with the fiber size, CEC, surface area, and water absorption. The results further indicated that sepiolites with low crystallinity or high level of surface silanol groups (K3 and B sepiolites) show the best rheological properties.

**Keywords:** sepiolite, rheology, crystallinity, pH

### 1. Introduction

Palygorskite-sepiolite group of clay minerals has a wide range of industrial applications stemming mainly from its sorptive, rheological, and catalytic properties (Alvarez et al., 2011; Zheng et al., 2011). These main properties are controlled by the extent of fibrous structure, surface area, porosity, crystal morphology, and chemical composition (Galan, 1996). The rheological properties of sepiolite render it valuable as a thickening, suspending, or thixotropic agent where a spectrum of diverse applications stretches from the manufacture of cosmetics and pharmaceutical products to that of paints and even fertilizers (Maqueda et al., 2008; Carmona et al., 2018).

Rheology is described as the flow of fluids and deformation of solids under applied stresses or strains and is concerned with the relationship between shear stress, shear strains, and time. There are two types of flow, Newtonian and non-Newtonian. In Newtonian flow (such as water or oil), viscosity is independent of shear rate. These flows show a linear relationship between shear rate and shear stress. Newtonian materials are featured by a constant viscosity at different shear rate. Non-Newtonian flow is the opposite of Newtonian flow. When a shear is applied, the viscosity of the non-Newtonian flow decreases or increases, depending on the type of flow. There are four different types of flow in non-Newtonian flow. These are dilatant, pseudo plastic, rheopectic, and thixotropic. Clays, polymers, and many similar materials are examples of non-Newtonian flow. The rheology of clay suspensions is determined with the help of rheological parameters such as viscosity (mPa), Torque

(%), shear stress (mPa), and shear rate ( $s^{-1}$ ). Different rheometers are used to determine these rheological parameters (Yahia et al., 2016).

Sepiolite is often found associated with other clays and non-clay minerals such as carbonates, quartz, feldspar, and phosphates. The structure of sepiolite includes three types of active sorption sites: (a) oxygen ions on the tetrahedral sheet of the ribbons, (b) water molecules coordinated to  $Mg^{2+}$  ions at the edges of structural ribbons (two  $H_2O$  molecules per  $Mg^{2+}$  ion), and (c) SiOH groups along the fiber axis (Serratosa, 1979). The structure and morphology of sepiolite particles cause the presence of a large number of terminal silica tetrahedra at the external surfaces. Silanol (Si-OH) groups are produced by broken Si-O-Si bonds which compensate for their residual charge by accepting a proton or hydroxyl group. These silanol groups occur at intervals of approximately 5Å along the particle axis (Tartaglione et al., 2008; Ovarlez et al., 2011), and play a major role in the displayed properties of sepiolite. The abundance of silanol groups in sepiolite is related to fiber dimensions and imperfections of the crystalline lattice (Santaren, 1993; Galan, 1996), which can be useful sites for chemical reactions (Bilotti et al., 2014).

Sepiolite is composed of countless large bundles of needle-like particles. Due to its low cation exchange capacity and chain-like structure, sepiolite does not swell when dispersed in water (Tartaglione et al., 2008; Lima et al., 2017). However, if the bundles of sepiolite particles are dispersed by mechanical mixing, many of the single particles are dragged from the bundles and entangle with other individual particles and bundles, forming a randomly intermeshed network that entraps liquid and increases the viscosity. In this condition, most water is held between particles and adsorbed on external and internal particle surfaces (Alvarez, 1984; Santaren, 1993). This structure is maintained by different forces between particles including van der Waals and hydrogen bonding through silanol groups. Anisometry of sepiolite particles also maintains the structure by mechanical entanglement which prevents settling to a closely packed structure (Santaren, 1993).

The cation exchange capacity (CEC) data of sepiolite samples offered in the literature vary greatly (4-40 meq/100 g) (Alvarez, 1984; Galan, 1996; Brigatti et al., 2006; Helmy and Bussetti, 2008; Maqueda et al., 2009; Verge et al., 2013; Olivato et al., 2015). These differences are usually attributed to the different crystalline compositions of the sepiolites. The CEC is due to the deficiency of charge caused by  $Si^{4+}$  substitution with trivalent ions that are internally compensated to a great degree, and to the existence of broken bonds at the edges of the fiber which give rise to unsatisfied charges that could be balanced by adsorbed cations. Broken bonds are possibly an important cause for the exchange capacity of sepiolite, especially in the more crystalline sepiolites (Grim, 1968; Alvarez, 1984; Galan, 1996).

The relative abundance of silanol groups in sepiolite has been suggested as a measure of the degree of crystallinity of this mineral (Ahlrichs et al., 1975). The low intensity of the SiOH band in palygorskite indicates less edge surface or fewer imperfections than observed for the several sepiolites. While the surface areas of sepiolite samples around the world are about 350  $m^2/g$  (Turker et al., 1997), 320  $m^2/g$  (Alvarez et al., 2011), between 125  $m^2/g$  and 458  $m^2/g$  (Gonzalez-Pradas et al., 2005), 311.5  $m^2/g$  (Helmy and Bussetti, 2008), 340  $m^2/g$  (Maqueda et al., 2009), between 83  $m^2/g$  and 343  $m^2/g$  (Cervini-Silva et al., 2017), palygorskite has the lower specific surface area as 195  $m^2/g$  (Barrer and Mackenzie, 1954) and 150  $m^2/g$  (Alvarez et al., 2011). The difference in surface areas between the two minerals is probably due to the difference in physico-chemical properties of their surfaces or palygorskite compared to sepiolite has fewer imperfections or fewer exposed edges (Serna et al., 1977; Cervini-Silva et al., 2017).

The identification of structural and textural differences between sepiolite minerals allows for a better understanding of the differences in the possible technological behaviors such as sorptive, rheological, and catalytic properties that are effective during its industrial applications. The differences in crystallinity of clay minerals can be explained by XRD analysis, thermal gravimetric analysis, FTIR spectra, surface area measurements, and microporosity and macroporosity measurements. XRD is used not only to define the creation of clay minerals but also to follow the crystallinity through changes in peak height and shape (Pickering, 2014). The decrease in XRD peak height and area of clay minerals, whereas the increase in the value of FWHM (Full Width at Half Maximum) is an indication of the decrease in crystallinity (Franco et al., 2014). The increase in

sharpening and intensity of peaks indicates the increase in the crystallinity of the clay. Crystallinity refers to the degree of structural order and arrangement of atoms or molecules in a solid (Bricker et al., 1973). The crystallinity index of kaolinite from clay minerals was calculated with the Hinckley index (*HI*). If *HI* > 1 of kaolinite is ordered, *HI* < 1 is defined as disordered. The XRD peak height was used to calculate the *HI* index (Hu and Yang, 2013).

The change in the crystallinity of clay minerals has also been demonstrated by DTA and TG studies by various researchers. Kaolinite (Hu and Yang, 2013) and sepiolite (Suarez and Garcia-Romero, 2012; Pozo Et al., 2014) were found to be similar to the results obtained from the XRD analysis. The change in endothermic peak temperatures of different clays is due to the change in their crystallinity. Clays with low crystallinity lost the crystal water at a lower temperature, while the higher the crystallinity of clays lost at a higher temperature. The results of the analysis of different kaolinites demonstrated a correlation between crystallinity and order degree, thermal stability, morphology, and surface characteristics of kaolinite (Hu and Yang, 2013).

This study aimed to identify differences in the rheological properties of sepiolite specific to Sivrihisar region of Turkey and correlate the chemical and mineralogical features of sepiolite with its technological properties.

## 2. Materials and methods

In this study, raw brown (K1, K2, and K3) and beige colours (B) sepiolite samples obtained from MAYAS Company in Eskisehir, Turkey were used for the experiments. The brown samples can be distinguished by their brown color with naked eyes. The chemical analyses of sepiolite used in this study are presented in Table 1. The chemical analysis was made by Inductively Coupled Plasma (ICP) in the ACME laboratory of Canada. The mineralogical analysis was made by Shimadzu XRD-6000 equipped with Cu K $\alpha$  X-rays.

The sepiolite samples (K1, K2, and K3) were crushed to less than 5 mm, and then the sepiolite suspensions were prepared at 3% by weight with distilled water and then ground in a ceramic ball mill (Mertest LB 220, Turkey) for 30 min. The mill inner dimensions are L=18.5 mm and R=15.5 mm, and the ball sizes used as the grinders were chosen as 30, 20, and 10 mm. Gel formation in sepiolite suspensions was induced before the viscosity measurements. The viscosity measurements were performed by a Brookfield, RVDV-II model spinning disc programmable viscometer operated at 5 rpm constant speed.

Two different methods were utilized because the first method aimed to reveal the change in apparent viscosity of sepiolite suspensions at constant rpm, and in the case of the second method, the change in the rheological properties of sepiolite suspensions. In the first method, suspensions of 3% by weight were prepared in 500 cm<sup>3</sup> volume and then transferred to a 600 cm<sup>3</sup> beaker in which viscosity measurements were conducted using RV1-2-3 spindles; these measurements are considered to be the only apparent viscosity values. It was observed that mixing the suspensions at a high speed of 17500 rpm for 10 min was observed to absorb heat and raise the temperature of the suspension to 35-40°C. Therefore, all suspensions were cooled down at room temperature for 10 min until the temperature of the suspension was brought to 25±1°C at which viscosity measurements were performed.

The second method involved the use of a small sample cell equipped with an SC-21 cylindero-conical-shaped mill. The temperature of suspension was maintained at the desired temperature (25±1°C) by a heat jacket which allowed the circulation of water around the cell. A volume of 8 cm<sup>3</sup> suspension was sufficient to perform each test. In addition to the apparent viscosities, in this set of measurements, shear stress (Pa) and shear rate (s<sup>-1</sup>) values were also recorded for more detailed data analysis. Since sepiolite suspensions exhibit a time-dependent flow pattern of thixotropy, the viscosity measurements were recorded versus time for 30 min. For interpretation, the value at the 15<sup>th</sup> min was selected according to the method presented elsewhere (Çınar, 2005; Çınar et al., 2009). In both methods, the ground sample taken out of the mill was subjected to blending at 17500 rpm for 10 min before the viscosity measurements.

While the pH profile of the sepiolite was being drawn, after the pH of the pure water was adjusted to 3 using HCl acid, sepiolite was added to the medium and the pH profile of the sepiolite suspension was obtained by monitoring the change in the pH of the medium over time. The pH of the suspension

was adjusted by analytical grade HCl (Merck) and recorded using a digital Orion pH meter. Cation exchange capacity (CAC) measurements for the samples were conducted in accordance with the API standards using the methylene blue test. Water absorption tests were performed by calculating the amount of water absorbed by a 20 g sample on a dry basis in the particle size range of 1 to 4 mm.

Jeol JSM-6335F scanning electron microscope (SEM) was used to determine the microstructure of sepiolite gels and sepiolite fiber size. Surface area measurements for the samples were performed with the Quantachrome Monosorb surface area analyzer.

The particle sizes of sepiolite samples were determined by the Fritsch Analysette 22 compact particle sizer analyzer. The sepiolite samples were dispersed in distilled water and stirred at a constant temperature of 20°C. The data collected were evaluated by the Fritsch software according to Fraunhofer diffraction theory. The average effective particle diameters ( $d_{50}$ ) of the sepiolite particles were determined.

Table 1. Chemical analyses of sepiolite samples

ELEMENT		K1	K2	K3	B
<i>SiO<sub>2</sub></i>	(%)	51.29	45.75	50.61	48.82
<i>Al<sub>2</sub>O<sub>3</sub></i>	(%)	1.37	1.37	1.99	1.17
<i>Fe<sub>2</sub>O<sub>3</sub></i>	(%)	0.58	0.59	0.81	0.51
<i>MgO</i>	(%)	22.57	21.89	21.34	22.28
<i>CaO</i>	(%)	0.26	3.31	0.28	1.17
<i>Na<sub>2</sub>O</i>	(%)	0.09	0.09	0.16	0.01
<i>K<sub>2</sub>O</i>	(%)	0.21	0.22	0.36	0.19
<i>TiO<sub>2</sub></i>	(%)	0.08	0.08	0.11	0.07
<i>Ba</i>	(ppm)	69	68	167	62
<i>Ni</i>	(ppm)	25	20	26	44
<i>Sr</i>	(ppm)	44	383	50	239
<i>Zr</i>	(ppm)	10	10	18	20
<i>Nb</i>	(ppm)	10	10	10	10
* <i>LOI</i>	(%)	23.6	26.2	24.6	25.7
<i>Tot. C</i>	(%)	0.38	1.87	0.31	0.60
<i>Tot. S</i>	(%)	0.03	0.02	0.01	0.02
<i>Tot.</i>	(%)	100.13	99.62	100.37	100.0
<i>Sepiolite</i>	(%)	91.13	77.50	86.16	86.12
<i>Dolomite</i>	(%)	-	10.88	-	3.84
<i>Others</i>	(%)	8.87	11.62	13.84	10.04

\*LOI: loss on ignition

### 3. Results and discussion

#### 3.1. pH profile of sepiolite suspensions

pH profiles of three different sepiolites at 3% solids concentration are shown in Fig. 1 which shows the pH profile of sepiolite suspensions for pH 3 as a function of time. As seen in Fig. 1, when the initial pH value of suspension is adjusted to 3.0, all four sepiolite samples attain equilibrium pH at different times. While K1 sepiolite reached the buffer pH (8.77) in approximately 4 min; K3 (pH 8.45) in 2 min; B sepiolite (pH 8.74) in 1 min. The reason for sepiolite suspensions reaching the buffer pH so quickly can be attributed to the release of Mg<sup>2+</sup> ions in the octahedral sheet and the rapid absorption of H<sup>+</sup> ions in water onto the surface of sepiolite (Sabah, 1998; Alkan et al., 2005). Sepiolite carries negative charges at the basic surfaces as a result of isomorphism. Since the ratio of isomorphous substitutions in sepiolite is low, its cation exchange capacity and the amount of negative charge on the permanent surface are low (Alvarez, 1984). Due to the discontinuity of silicate layers on sepiolite (Darder et al., 2006; Duquesne et al., 2007; García-Lopez et al. 2010; Olivato et al., 2015), the balance of charge is supplied by the silanol groups located near the channels which form as a result of broken fibers and in

turn, displays the Si-O-Si bonds on the fiber surfaces; these sites break and provide the required protons and hydroxyl groups. The abundance of silanol groups in sepiolite is related to crystallinity, fiber dimensions, surface area, and imperfections of the crystalline lattice (Ahlrich et al., 1975; Serna et al., 1977; Alvarez, 1984; Simonton, 1988; Santaren, 1993; Hibino et al., 1995; Galan, 1996; Suarez and Garcia-Romero, 2012).

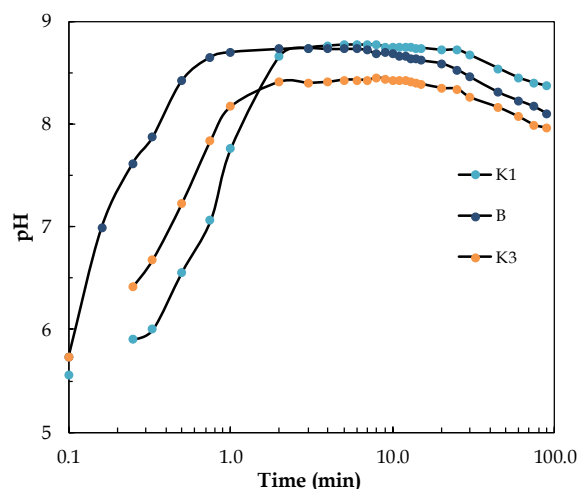


Fig. 1. pH profiles of different sepiolites as a function of time

Owing to these reasons, it is thought that the amount of energy required to break Si-O-Si bonds and to achieve the isomorphous substitution among different sepiolites will be different. Therefore, it can be envisaged that the lower surface area (Table 2), the degree of isomorphous substitution, and its better crystallinity of K1 sepiolite require more energy in breaking the bonds; this results in the slower adsorption of  $H^+$  ions in the medium. In the same context, with a relatively slower decline in pH profile and its prolonged existence, K1 sepiolite exhibits slow ion exchange. As opposed to this, it was perceived that the other three sepiolites reached the final pH in a shorter time and exhibited better rheological characteristics compared to K1 sepiolite; the CEC and water adsorption tests carried out with these sepiolites confirm these results (Table 2).

Table 2. Cation exchange capacity (CEC), water adsorption, and surface area of different sepiolites

Sample	K1	K2	K3	B
CEC (meq/100 g)	17.42	16.39	25.61	24.59
Water ads. (%)	191.85	204.70	265.20	306.50
Surface area ( $m^2/g$ )	291	260	314	359

### 3.2. Rheological properties of sepiolites

It is envisaged that the aforementioned differences in colloidal properties can be reflected in the rheological properties of different sepiolites. Several rheological tests were performed on the sepiolite samples to find out the changes in shear stress -shear rate, viscosity-shear rate, thixotropy index, and time-dependent changes in viscosity.

For all sepiolite samples, the flow curves are typical of clay materials with a pseudo plastic behavior (van Olphen, 1977). At low shear rates, such systems exhibit non-Newtonian flow (Fig. 2), which is characterized by a progressive decline in viscosity as the shear rate increases (Fig. 3). Above a certain value of shear rate, the flow curve becomes linear (Fig. 2). Aqueous clay suspensions that possess relatively high particle concentrations are traditionally described following the Bingham theory of plastic flow (Bingham, 1922; Güven, 1992; Alan and Işçi, 2014; Carmona, et al., 2018). All sepiolite samples and aqueous sepiolite suspensions prepared at low solids (3% w/w) concentrations displayed plastic flow behavior similar to the systems with high concentrations and conformed to the generalized Bingham plastic flow model (Figs. 2 and 3). According to this model, the slope of the

linear part of the flow curve (Fig. 2) refers to the plastic viscosity and the intercept of the linear portion of the curve with the stress axis refers to the Bingham yield (stress) value. Another rheological parameter is the apparent viscosity, which is defined as the ratio of shear stress/to the shear rate at any shear rate. In our study, the apparent viscosity was obtained at a shear rate of  $93 \text{ s}^{-1}$ . The values of plastic viscosity, Bingham yield value, thixotropic index, and apparent viscosity are presented in Table 3.

The individual fibers of sepiolite are associated with network structures of micro-aggregates ( $<250 \mu\text{m}$ ). The network structure progressively breaks down as the rate of shear increases, leading to an overall decrease in viscosity (Fig. 3). There is a certain shear rate at which structural disruption is complete, and above which the viscosity remains constant (Fig. 3). Viscosity is a measure of the resistance to the flow of individual fibers of sepiolite, while yield stress represents the work required to break down the network structures.

Table 3. Plastic viscosity, apparent viscosity, Bingham yield stress, and thixotropic index (2.5 rpm viscosity value / 20 rpm viscosity value) of sepiolite suspensions at 3% (w/v)

Samples	Plastic Viscosity (mPa.s)	Apparent Viscosity (mPa.s)	Bingham Yield Stress (Pa)	Thixotropic Index (2.5 rpm/20 rpm)
K1	1.40	38.49	3.45	6.54
K2	2.31	75.48	6.80	6.13
K3	25.26	199.46	16.20	5.95
B	40.86	143.55	15.60	5.49

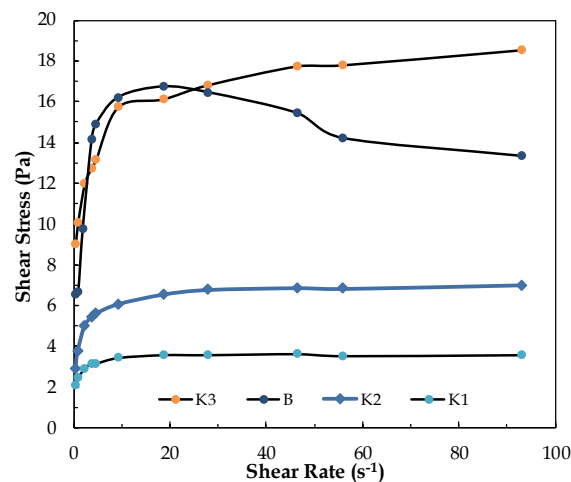


Fig. 2. Flow properties of different sepiolite suspensions at 3% w/w

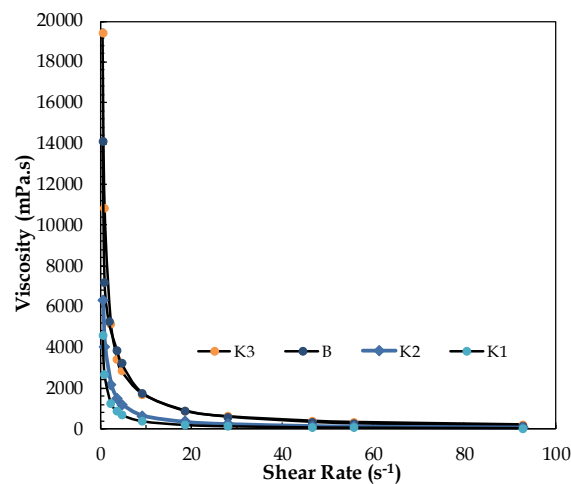


Fig. 3. Viscosity versus shear rate rheograms of different sepiolite suspensions

Clay suspensions frequently show a time-dependent flow behavior, known as thixotropy (van Olphen, 1977, Luckham and Rossi, 1999; Tunç et al., 2011). The network structure of the semi-rigid gel appears to be broken by shear forces and the inter-particle bonds tend to re-establish themselves with time (Güven, 1992; Neaman and Singer, 2000; Tunç et al., 2011). In other words, from a rheological point of view, thixotropy is defined as the isothermal and reversible gel-liquid transformation upon mechanical agitation (Güven, 1992). A thixotropic system begins to flow under stirring and thickens again when standing. Such a suspension will change during flow curve measurements by a viscometer, and a hysteresis loop shown in Fig. 4 will be obtained, upon subsequently taking readings at increasing and decreasing shear rates (Luckham and Rossi, 1999; Neaman and Singer, 2000). Additionally, when the clay system is subjected to a constant shear rate, the viscosity decreases with time because the gel structure is broken down until equilibrium viscosity is reached (Fig. 5). The decrease in the viscosity values against time presented in Fig. 5 clearly shows that sepiolite suspensions also exhibit thixotropic properties. Due to their shear and time dependency, if comparisons are to be made between the rheological properties of different samples, the clay suspensions require the same preparation, handling, and measurement conditions (Luckham and Rossi, 1999).

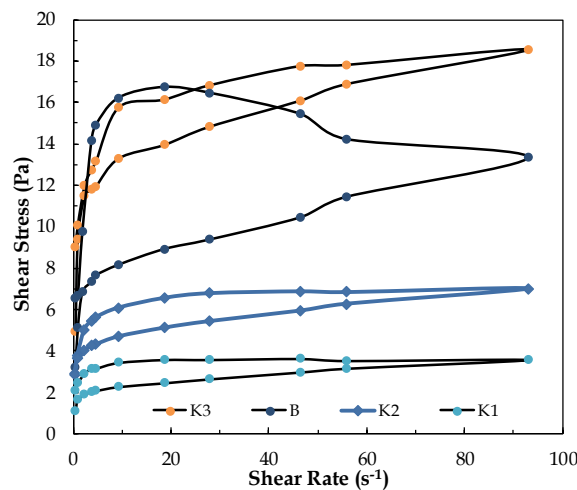


Fig. 4. Flow properties of 3% w/w sepiolite suspensions showing thixotropic behavior and hysteresis

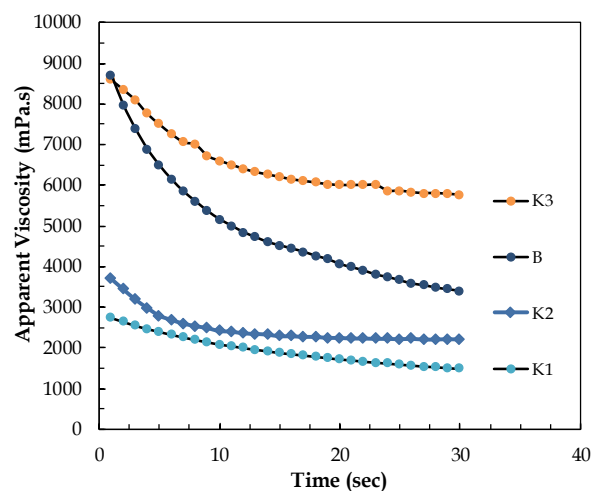


Fig. 5. Viscosity versus time rheograms of sepiolite suspensions demonstrating their thixotropic behavior (Brookfield viscosity at 5 rpm with spindle RV-1-2-3)

The apparent viscosity values decrease with an increase in the shear rate “shear-thinning” (Fig. 3). The change in the thixotropy of sepiolite samples given in Fig. 4 follows the order of  $B > K3 > K2 > K1$ . In terms of apparent viscosity values; however, this occurs as  $K3 > B > K2 > K1$  (Fig. 5).

### 3.3. XRD and SEM analyses of sepiolites

XRD analyses of sepiolite samples wet ground for 30 min in a ceramic ball mill at the ratio of 3% (w/w) are seen in Fig. 6 whereas the corresponding SEM photographs are also shown in Fig. 7. Quasi-quantitative analysis was carried out with the help of XRD and chemical analyses (Table 1) K1>90%, K3, and while the sepiolite content of B sepiolite is over 85%, it is below 80% for K2. It was found that the  $d_{50}$  sizes measured after 10 min blending at 3 % (w/w) are similar for K2 (6.49  $\mu\text{m}$ ), K3 (6.15  $\mu\text{m}$ ), and B (4.75  $\mu\text{m}$ ) sepiolites. As opposed to this, the value of 10.16  $\mu\text{m}$  measured for K1 is rather different. This demonstrates that the fibers of K1 sepiolite cannot be easily liberated from their associated bundles. The XRD analysis of sepiolite was further used to determine the crystallinity of the samples and the presence of crystalline impurity phases. The measure of crystallinity was taken from approaches that appeared in the literature (Brindley, 1959; Bricker et al. 1973; Germine, 1987; Hu and Yang, 2013; Pickering, 2014; Franco et al., 2014).

In summary, the best crystallinity followed the order of K1>K2>B>K3 whereas contrary to crystallinity, the rheological properties of the sepiolite suspensions exhibited the order of K3>B>K2>K1. There is an inverse relationship between the degree of crystallinity and rheological properties. Ahlrichs et al. (1975) in this context showed that the number of silanol groups on the surface of a sepiolite fiber is dependent upon the crystallinity of the fiber. They found that the better-crystallized samples contained the fewest number of surface silanol groups and the poorly crystallized sample the greatest number. Of the sepiolites used in this study, the XRD (Fig. 6) analysis showed that the K1 sepiolite was well-crystallized, whereas the K2 sepiolite was moderately crystallized and the K3 and B sepiolites were poorly crystallized; this indicated that the K3 and B sepiolites had a greater number of silanol groups per surface area than the others.

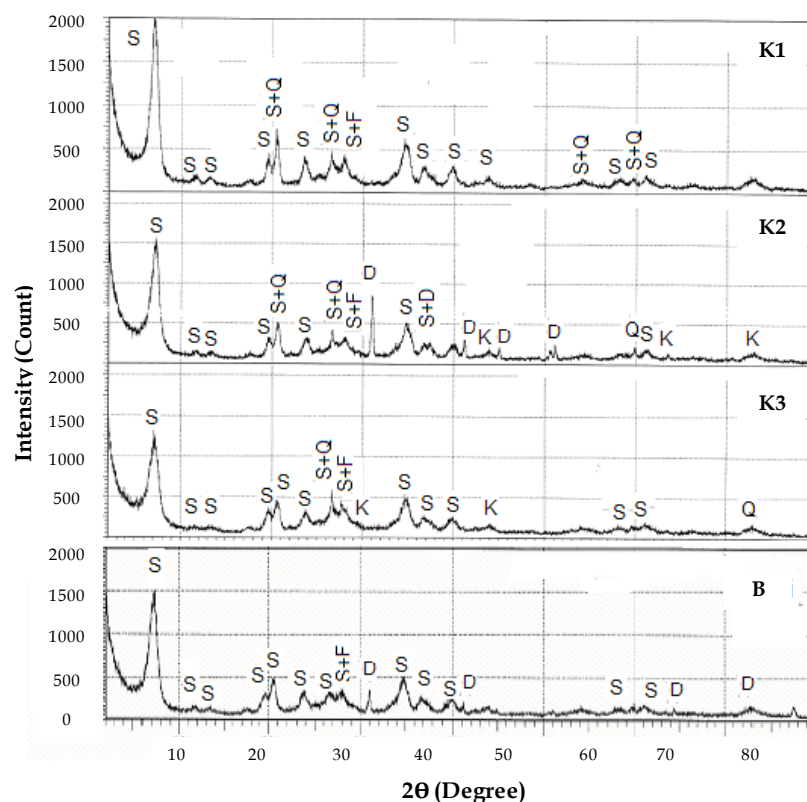


Fig. 6. XRD spectra of sepiolite samples (K1, K2, K3, and B) (S: Sepiolite; D: Dolomite; Q: Quartz; K: Calcite; F: Feldspar; I: Illite)

The exact mechanism of gelling in sepiolite is not well-understood, but the results of this study suggest that silanol groups on the surface of the sepiolite fibers play an important role in arranging fibers together such that the gel structures can develop. The differences in the flow curves of sepiolite suspension are related to the size and shape of individual sepiolite fibers. In this study, the size and



shape of individual particles were determined by Scanning Electron Microscopy (SEM) to confirm the hypothesis (Fig. 7). The results indicate that the samples were different from each other in length and width of the fibers for all samples. SEM photos which were magnified 5000 times demonstrated that the fiber length and width of the samples differed from each other.

According to Güven (1992), nonspherical forms are described as an ellipsoid. The ellipticity of fibers is defined as the  $L/W$  ratio where  $L$  is the length and  $W$  is the width of the fibers. The examination of the effect of fiber ellipticity on rheological properties for sepiolite suspensions reveals that rheological properties increase with increasing the ellipticity of fibers. This increase takes place as a result of the free fibers' in sepiolite suspension forming a network structure. As can be seen from the SEM photos given in Fig. 7, B and K3 sepiolites exhibit longer (nearly  $5\ \mu\text{m}$ ) and narrower fibers whereas K1 sepiolite shows shorter (nearly  $3\ \mu\text{m}$ ) but wider. The ratio of length ( $L$ ) and width ( $W$ ) is high for B and K3 sepiolites, and narrower for K1 sepiolite. Increasing this ratio causes expansion in the rheological properties of sepiolite suspensions. (Simonton et al., 1988; Güven, 1992; Neaman and Singer, 2000; Franco et al., 2014). The number of silanol groups located at the external surface of sepiolite is influential on the rheological properties (Simonton et al., 1988). The relative abundance of these groups in sepiolite is related to the dimension of the particle and imperfections of the crystalline lattice (Alvarez, 1984; Santaren, 1993). This has been suggested as a measure of the degree of crystallinity of sepiolite (Ahrichs et al., 1975). In a study conducted by Aznar et al. (1992), the reasons for the decrease in viscosity of sepiolite were ascribed to the progressive coverage of the sepiolite surface by Methylene blue. Methylene blue adsorption on the sepiolite avoids particle-particle interactions. The decrease in viscosity is parallel to the perturbation of the silanol groups on the sepiolite surface. This distortion also affects charge balance and particle-to-particle interactions. Inter-particle forces are stronger in the case of sepiolite, as well as the capacity to immobilize liquid, thereby yielding higher viscosities (Santaren, 1993).

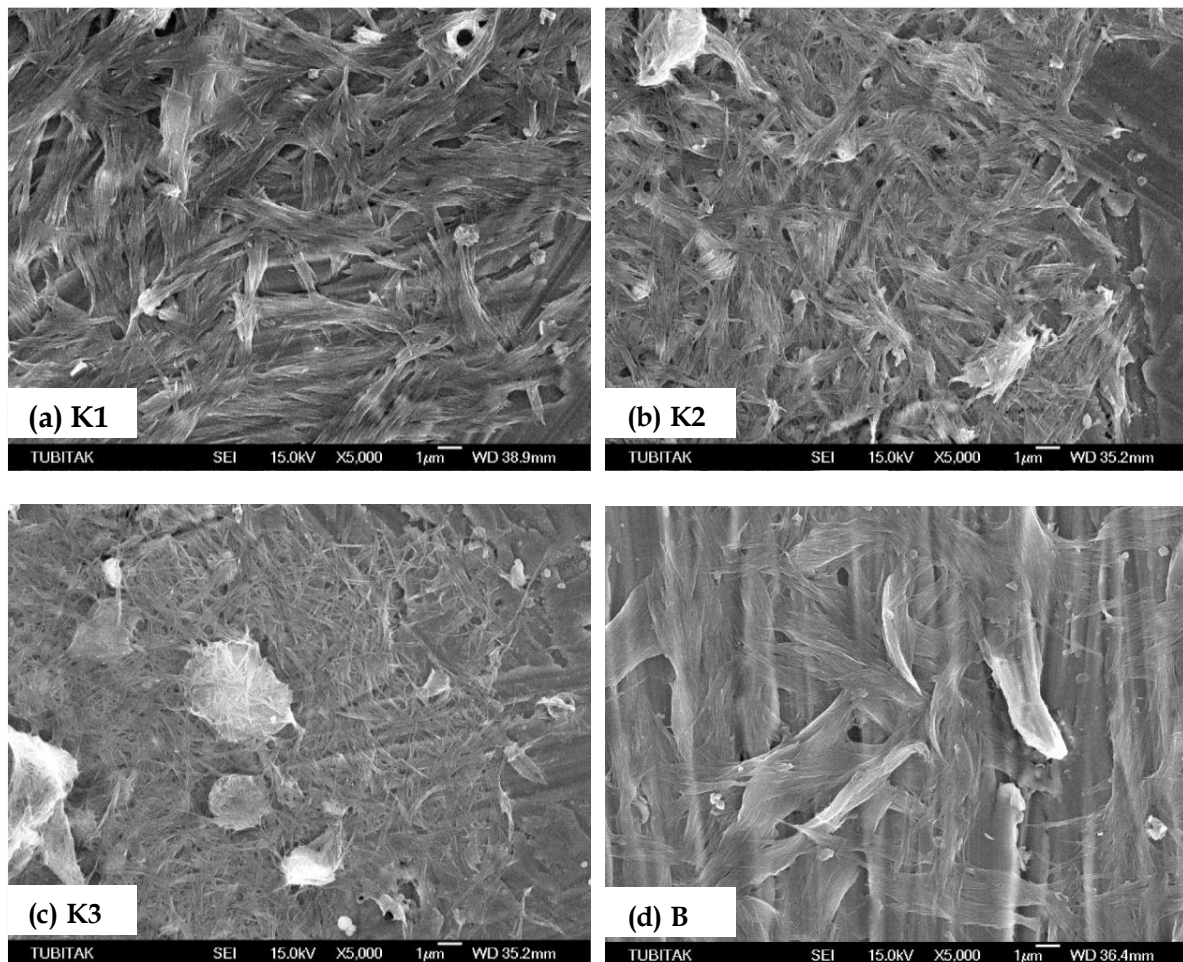


Fig. 7. SEM photographs of sepiolite samples (a) K1, (b) K2, (c) K3, and (d) B

Similar differences can be seen in cation exchange capacity, water adsorption and surface area carried out with various sepiolites examined in this study, as presented in Table 2 which revealed that the K3, B sepiolite has a much greater *CEC*, water adsorption, and surface area than do other sepiolites (Hibino et al., 1995; Vicoso et al., 2009; Suarez and Garcia-Romero, 2012; Pozo et al., 2014). This may be due to a greater number of surface silanol groups than the others (Simonton et al., 1988). The fact that *CEC* (16.39 meq/100 g), water adsorption (204.7%), and surface area (260 m<sup>2</sup>/g) for K2 were low and similar to K1; this is caused by the fact that the impurity levels are relatively high compared to others. These values show that *CEC*, surface area, and water absorption are influential parameters on rheological properties.

To sum up, the number of silanol groups on the surfaces of sepiolite fibers is one of the most important reasons that affect the rheological properties of sepiolite. It is perceived that there is a direct positive correlation between the increase in the number of silanol groups, fiber dimensions or ellipticity, surface area, water adsorption, and *CEC* which were found to agree with the studies in the literature (Ahlrichs et al., 1975; Serna, 1977; Alvarez, 1984; Simonton et al., 1988; Santaren, 1993; Hibino et al., 1995; Galan; 1996; Neaman and Singer, 2000; Vicoso et al., 2009; Pozo et al., 2014; Franco et al., 2014).

#### 4. Conclusions

The relative abundance of silanol (SiOH) groups in sepiolite are suggested as a measure of the degree of crystallinity. The differences in SiOH groups found among different sepiolites are attributed to fiber dimensions, imperfections in the crystal lattice, crystallinity, and surface areas. The defects in the crystal lattice also affect the *CEC* and induce the following features.

- The degree of crystallinity plays a major role in the solubility and acid-base interactions in sepiolite (Franco et al., 2014) and resulted in the following order: B>K3> K2>K1
- All sepiolite suspensions, even at as low as 3% by wt., behave like concentrated systems and exhibited plastic flow behavior with thixotropy and follow the generalized Bingham Plastic Flow model.
- Differences found in the rheological properties among various sepiolites can be explained by the level of silanol groups, the level of impurities, and the degree of crystallinity. The rheological properties, similar to that of pH, follow the order as B>K3>K2>K1.

As a result, it was seen that the rheological measurements made to determine the rheological properties of different sepiolites are caused by the differences in the structural and morphological properties of the sepiolites and they affect the rheological properties. Differences in pH profiles, surface areas, XRD analyses, and SEM images of sepiolites revealed this situation. It is clear from these analyzes that the real reason for the difference in the rheological properties of sepiolites is that they have different crystallinity due to their formation.

#### Acknowledgments

The authors would like to acknowledge the financial support of TÜBİTAK-The Scientific and Technological Research Council of Turkey (Project Number: 104M179). We also would like to express our endless gratitude to our valuable teacher Prof. Mehmet S. Çelik, who has not spared all kinds of help throughout our academic life and has made great contributions to our scientific development starting from our student life.

#### References

- AHLRICH, J.L., SERNA, C., and SERRATASO, J.M., 1975. *Structural hydroxyls in sepiolites*. Clays and Clay Minerals, 23: 119-124.
- ALAN, N., İŞÇİ, S., 2014. *Surface modification of sepiolite particles with polyurethane and polyvinyl alcohol*. Progress in Organic Coatings, 77: 444-448.
- ALKAN, M., DEMİRBAŞ, Ö. and DOĞAN, M., 2005. *Electrokinetic properties of sepiolite suspensions in different electrolyte media*. Journal of Colloid and Interface Science, 281: 240-248.

- ALVAREZ, A., 1984. *Sepiolite: Properties and Uses*, In: *Palygorskite-sepiolite occurrences, genesis and uses*. Editors Singer, A. and Galan, E., *Developments in Sedimentology*. 37: Elsevier, Amsterdam, pp. 253-287.
- ÁLVAREZ, A., SANTARÉN, J., ESTEBAN-CUBILLO, A., and APARICIO, P., 2011. *Current industrial applications of palygorskite and sepiolite*. Editors Emilio Galan and Arieh Singer. *Developments in Clay Science*. 3: Elsevier, Amsterdam, The Netherlands. pp. 281-298.
- AZNAR, A.J., CASAL, B., RUIZ-HITZKY, E., LOPEZ-ARBELOA, F., SANTAREN, J. and ALVAREZ, A., 1992. *Adsorption of methylene blue on sepiolite gels: Spectroscopic and rheological studies*. *Clay Minerals*, 27: 101-108.
- BARRER, R.M. and MACKENZIE, N., 1954. *Sorption by attapulgite: Part I. availability of intracrystalline channels*. *Journal of Physical Chemistry*, 58: 560-567.
- BILOTTI, E., DUQUESNE, E., DENG, H., ZHANG, R., QUERO, R., GEORGIADIS, S.N., FISCHER, H.R., DUBOIS, P., PEIJS, T., 2014. *In situ polymerised polyamide 6/sepiolite nanocomposites: Effect of different interphases*. *European Polymer Journal*, 56: 131-139.
- BINGHAM, E.C., 1922. *Fluidity and Plasticity*. McGraw-Hill.
- BRICKER, O.P., NESBITT, H.W., GUNTER, W.D., 1973. *The stability of talc*. *American Mineralogist*, 58: 64-72.
- BRIGATTI, M.F., GALAN, E., THENG, B.K.G., 2006. *Structures and mineralogy of clay minerals*. In: Eds. Bergaya, F., Theng, B.K.G., Lagaly, G., *Handbook of Clay Science*. *Developments in Clay Science*, Vol. 1, Amsterdam, Elsevier, pp. 19-86.
- BRINDLEY, G.W., 1959. *X-ray and electron diffraction data for sepiolite*. *The American Mineralogist*, 44: 495-499.
- CARMONA, J.A., RAMÍREZ, P., TRUJILLO-CAYADO, L.A., CARO, A., MUÑOZ, J., 2018. *Rheological and microstructural properties of sepiolite gels. Influence of the addition of ionic surfactants*. *Journal of Industrial and Engineering Chemistry*, 59: 1-7.
- CERVINI-SILVA, J., RAMIREZ-APAN, M.T., KAUFHOLD, S., PALACIOS, E., GOMES-VIDALES, V., UFER, K., ANGEL, P., MONTOYA, A., 2017. *Cell growth underpinned by sepiolite*. *Applied Clay Science*, 137: 77-82.
- ÇINAR, M., 2005. *Rheologic characteristics of sepiolites' and water based sepiolite production*. Ph.D. Thesis, Istanbul Technical University, Istanbul, Turkey.
- ÇINAR, M., CAN, M.F., SABAH, E., KARAGÜZEL, C., ÇELIK, M.S., 2009. *Rheological properties of sepiolite ground in acid and alkaline media*. *Applied Clay Science*, 42: 422-426.
- DARDER, M., LOPEZ-BLANCO, M., ARANDA, P., AZNAR, A.J., BRAVO, J., RUIZ-HITZKY, E., 2006. *Microfibrous chitosan-sepiolite nanocomposites*. *Chemical Materials*, 18:1602-1610.
- DUQUESNE, E., MOINS, S., ALEXANDRE, M., DUBOIS, P., 2007. *How can nanohybrids enhance polyester/sepiolite nanocomposite properties*. *Macromolecular Chemistry and Physics*, 208: 2542-2550.
- FRANCO, F., POZO M., CECILIA, J.A., BENITEZ-GUERRERO, M., POZO, E., MARTIN RUBI, J.A., 2014. *Microwave assisted acid treatment of sepiolite: The role of composition and "crystallinity"*. *Applied Clay Science*, 102: 15-27.
- GALAN, E., 1996. *Properties and applications of palygorskite-sepiolite clays*. *Clay Minerals*, 31: 443-453.
- GARCÍA-LOPEZ, D., FERNÁNDEZ, J.F., MERINO, J.C., SANTARÉN, J., PASTOR, J.M., 2010. *Effect of organic modification of sepiolite for PA 6 polymer/organoclay nanocomposites*. *Composites Science and Technology*, 70: 1429-1436.
- GERMINE, M., 1987. *Sepiolite asbestos from Franklin, New Jersey: A case study in medical geology*. *Environmental Research*, 42: 386-399.
- GONZALEZ-PRADAS, E., SOCIAS-VICIANA, E., URENA-AMATE, M.D., CANTOS-MOLINA, A., VILLAFRANCA-SANCHEZ, M., 2005. *Adsorption of chloridazon from aqueous solution on heat and acid treated sepiolites*. *Water Research*, 39: 1849-1857.
- GRIM, R.E., 1968. *Clay Mineralogy (2nd Ed.)*. McGraw-Hill, New York, CO. pp. 596.
- GÜVEN, N., 1992. *Rheological aspects of aqueous smectite suspensions*. Eds. Güven, N. and Pollastro, R.M., *Clay-water interface and its implications*. *Clay Min. Soc. Workshop Lectures*, The Clay Minerals Society, 4: 81-125.
- HELMY, A.K., BUSETTI, S.G., 2008. *The surface properties of sepiolite*. *Applied Surface Science*, 255: 2920-2924.
- HIBINO, T., TSUNASHIMA, A., YAMAZAKI, A., OTSUKA, R., 1995. *Model calculation of sepiolite surface areas*. *Clays and Clay Minerals*. 43: 391-396.
- HU, P., YANG, H., 2013. *Insight into the physicochemical aspects of kaolins with different morphologies*. *Applied Clay Science*, 74: 58-65.
- LIMA, J. A DE., CAMILO, F.F., FAEZ, R., CRUZ, S.A., 2017. *A new approach to sepiolite dispersion by treatment with ionic liquids*. *Applied Clay Science*, 143: 234-240.

- LUCKHAM, P.F., ROSSI, S., 1999. *The colloidal and rheological properties of bentonite suspensions*. *Advances in Colloid and Interface Science*, 82: 43-92.
- MAQUEDA, C., VILLAVERDE, J., SOPEÑA, F., UNDABEYTIA, T., MORILLO, E., 2008. *Novel system for reducing leaching of the herbicide metribuzin using clay-gel-based formulations*. *Journal of Agricultural Food Chemistry*, 56 (24): 11941-11946.
- MAQUEDA, C., PARTAL, P., VILLAVERDE, J., PEREZ-RODRIGUEZ, J.L., 2009. *Characterization of sepiolite-gel-based formulations for controlled release of pesticides*. *Applied Clay Science*, 46: 289-295.
- NEAMAN, A. and SINGER, A., 2000. *Rheological properties of aqueous suspensions of palygorskite*. *Soil Science Society American Journal*, 64: 427-436.
- OLIVATO, J.B., MARINI, J., POLLET, E., YAMASHITA, F., GROSSMANN, M.V.E., AVÉROUS, L., 2015. *Elaboration, morphology and properties of starch/polyesternano-biocomposites based on sepiolite clay*. *Carbohydrate Polymers*, 118: 250-256.
- OVARLEZ, S., GIULIERI, F., DELAMARE, F., SBIRRAZZUOLI, N., CHAZE, A.M., 2011. *Indigo-sepiolite nanohybrids: Temperature-dependent synthesis of two complexes and comparison with indigo-palygorskite systems*, *Microporous and Mesoporous Materials*, 142: 371-380.
- PICKERING, R.A., 2014. *Tri-octahedral domains and crystallinity in synthetic clays: implications for lacustrine paleoenvironmental reconstruction*. Master Thesis, College of Arts and Sciences Georgia State University.
- POZO, M., CALVO, J.P., POZO, E., MORENO, A., 2014. *Genetic constraints on crystallinity, thermal behaviour and surface area of sepiolite from the cerro de los batallones deposit (Madrid basin, Spain)*. *Applied Clay Science*, 91-92: 30-45.
- SABAH, E., 1998. *Adsorption mechanism of various amines onto sepiolite*. Ph.D. Thesis, Osmangazi University, Eskişehir, Turkey.
- SANTAREN, J., 1993. *Sepiolite: a mineral thickener and rheology additive*. *Modern Paint and Coatings*. 98-72.
- SERNA, C., VANSOYOC, G.E. and AHLRICH, J.L., 1977. *Hydroxyl groups and water in palygorskite*. *American Mineralogist*, 62: 784-792.
- SERRATOSA, J.M., 1979. *Surface properties of fibrous clay minerals (palygorskite and sepiolite)*. *Proceedings of the VI International Clay Conference 1978.*, Oxford, Elsevier. *Developments in Sedimentology*. 27: 99-109.
- SIMONTON, T.C., KOMARNENI, ROY, R. 1988. *Gelling properties of sepiolite versus montmorillonite*. *Applied Clay Science*, 3: 165-176.
- SUAREZ, M. and GARCIA-ROMERO, E., 2012. *Variability of the surface properties of sepiolite*. *Applied Clay Science*, 67-68: 72-82.
- TARTAGLIONE G., TABUANI D., CAMINO, G., 2008. *Thermal and morphological characterization of organically modified sepiolite*. *Microporous and Mesoporous Materials*, 107: 161-168.
- TUNÇ, S., DUMAN, O., ÇETINKAYA, A., 2011. *Electrokinetic and rheological properties of sepiolite suspensions in the presence of hexadecyltrimethylammonium bromide*. *Colloids and Surfaces A: Physicochemical Engineering Aspects*, 377: 123-129.
- TURKER, A.R., BAG, H., ERDOGAN, B., 1997. *Determination of iron and lead by flame atomic absorption spectrometry after preconcentration with sepiolite*. *Fresenius Journal of Analytical Chemistry*, 357: 351-353.
- VAN OLPHEN, H., 1977. *An introduction to clay colloid chemistry*. 2nd ed. John Wiley and Sons, New York.
- VERGE, P., FOUQUET, T., BARRERE, C., TONIAZZO, V., RUCH, D., BOMFIM, J.A.S., 2013. *Organomodification of sepiolite clay using bio-sourced surfactants: Compatibilization and dispersion into epoxy thermosets for properties enhancement*. *Composites Science and Technology*, 79: 126-132.
- VICOSA, A.L., GOMES, A.C.O., SOARES, B.G., PARANHOS, C.M., 2009. *Effect of sepiolite on the physical properties and swelling behavior of rifampicin-loaded nanocomposite hydrogels*. *Express Polymer Letters*, 3: 518-524.
- YAHIA, A., MANTELLATO, S., FLATT, R.J., 2016. *Concrete Rheology: A basis for understanding chemical admixtures*. *Science and Technology of concrete admixtures*. Eds., Aitcin, Pierre-Claude and Flatt R.J., 97-127.
- ZHENG, Y.P., ZHANG, J.X., LAN, L., YU, P.Y., 2011. *Sepiolite nanofluids with liquid-like behavior*. *Applied Surface Science*, 257: 6171-6174.